



# Investigation of the combined stress and strain situation in diffusion welded rectifying elements

O. Korolkov, T. Rang & R. Kurel

*Department of Electronics, Tallinn Technical University, Estonia*

## Abstract

During the post-bonding cooling process, and due to the differences in the thermal expansion coefficients of the bonded parts, thermal stresses and deformations arise in rectifying elements. The residual stresses and deformations may be the main factor in the subsequent technological treatments and operations. In early papers the regularities of the residual stress and strain situation in general, without examination of the stress distribution along the cross section of the rectifying element during the process of cooling, were observed. The subject of this paper is the use of the finite element method (FEM) and experimental data for investigation of the stress and strain kinetics of rectifying elements during the post-deposition welding cooling process.

## 1 Introduction

Diffusion welding (DW) is a solid state joining process, which can be utilized to bond "difficult to join" metals or dissimilar material combinations [1].

In the simplest form the DW process includes heating up to a temperature not above the melting point of any of contact materials and compression under a pressure not exceeding the breaking compressive strength of contact materials.

The process of diffusion welding has been known for many years, but only in the last time the application of DW was propagated to power electronics, in particular for metallization of semiconductor structures and bonding of power device heat sink electrodes [2]. The today's power semiconductor rectifying element has traditionally a very thin ( $250 \div 600 \mu\text{m}$  in thickness) semiconductor wafer bonded with heat sink electrode (tungsten or molybdenium with thickness of  $2 \div 4 \text{ mm}$ ) over thin ( $10 \div 100 \mu\text{m}$ ) plastic contacting metal (Fig. 1).

The dimensions of modern rectifying elements may be up to 4" diameter. So, the clear view of the stress and strain situation and the ability to control this situation is the essential necessity in the modern semiconductor rectifier production.

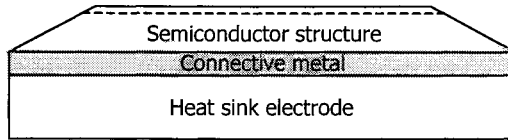


Figure 1: Schematic picture of power semiconductor rectifier.

## 2 Method

From the standpoint of mechanics, such a structure (Fig. 1) presents the axially symmetric multilayer composite cylinder comprising layers of elastic and plastic materials. In our case the diffusion welded model for rectifying element has the diameter 40 mm and it is formed on base of 0.6 mm thick silicon semiconductor wafer, bounded with 2 mm thick tungsten disc over 0.1 mm aluminium foil, which is chosen for the basic object in our investigations (Fig. 2).

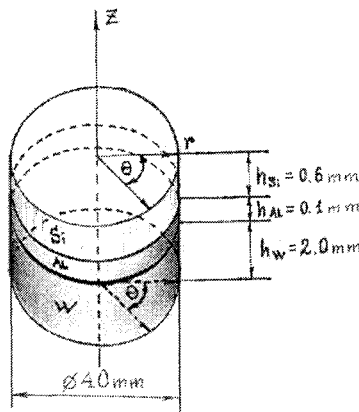


Figure 2: Schematic picture of the basic object in cylindrical coordinates.

For the calculations the Finite Element Method (FEM) was used and the cross-section of rectifying element was broken up into 320 elements with 187 junctions in the way as it is shown in Fig. 3.

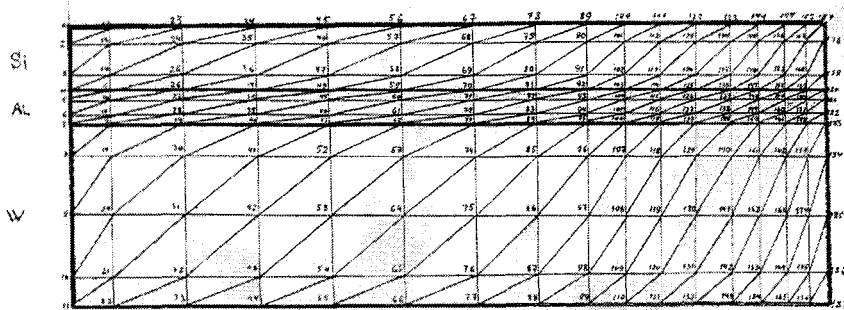


Figure 3: The discretisation picture of the rectifying element.

In the simulations the following assumptions were made. First W and Si were assumed to be elastically deformed over the whole thermo-mechanical stress field and their Young's modulus ( $E$ ) and the Poisson ( $\nu$ ), factor were assumed to be independent on temperature. Secondly, the aluminium layer was assumed to have only plastio-elastic deformations with negligible linear strengthening in all temperature regions and the creep of the aluminium is not taken into account.

The temperature dependences for main mechanical properties of the materials, going to be welded are shown in Fig. 4.

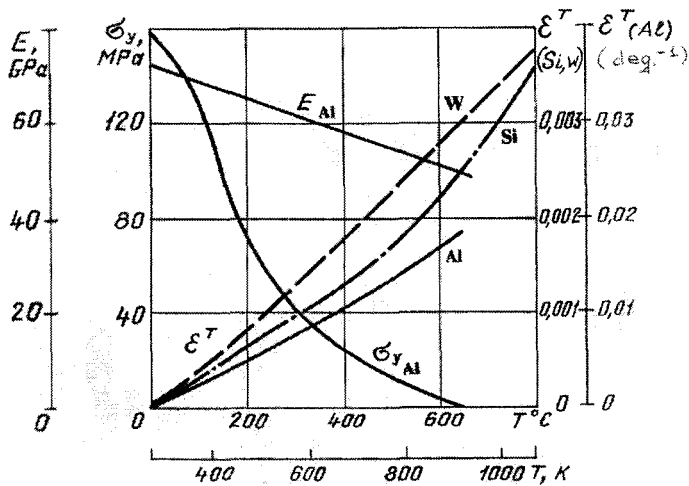


Figure 4: Variation of volume thermal expansion coefficient ( $\epsilon^T$ ), Young's modulus ( $E$ ) and yield stress ( $\sigma_y$ ) with the temperature.

### 3 Results

Figure 5 shows the temperature kinetics of radial stress in the cross-section of the rectifying structure.

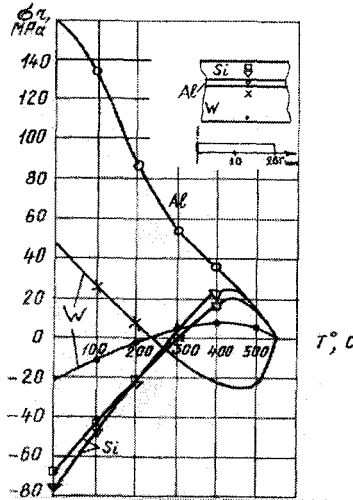


Figure 5: Radial stress ( $\sigma_r$ ) kinetics in the section  $r = 10\text{mm}$ .

In the initial cooling stage (from  $550^\circ$  to  $300^\circ\text{C}$ ) the Si wafer is under tensile radial stress due to higher rate of temperature change compared with W (Fig. 4). Starting from  $300^\circ\text{C}$  the compressive radial stresses rise in silicon and they will increase till the temperature reaches the room temperature. In the cooling of tungsten, the bonded face (from  $550^\circ$  to  $240^\circ\text{C}$ ) stays under the compressive stress, and the opposite (bottom) face will be under tensile stress. At the temperature  $240^\circ\text{C}$  the sign of the stresses changes into opposite. In silicon the minimum values of the stress correspond to the temperature close to  $300^\circ\text{C}$ . At the temperature  $240^\circ\text{C}$ , both tungsten and silicon, lose the stress gradient along the height of the rectifying structure and therefore the rectifying element has not bend deformation at this temperature. The residual stresses have maximum value at the room temperature for all of the layers of the rectifying element. The monotonous increase of tensile stress in aluminium is caused by the increase of its yield stress, when the temperature falls down.

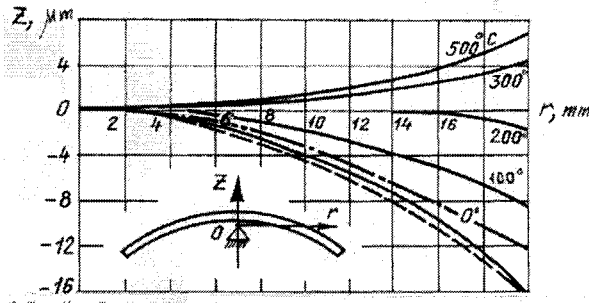


Figure 6: Bending flexure of rectifying element at different temperatures.

- FEM solution
- · - · - · experimental
- the ideal spherisity

In the beginning of the cooling process the bend flexure of rectifying element is negative and the changes are in accordance with the kinetic behavior of stresses. At the temperature lower then 240°C the bending flexure becomes a positive sign and at the room temperature the bend flexure has its maximum value (Fig. 6). The calculated and experimental data for bend flexure of rectifying element at room temperature are in a good conformity.

Fig. 7 shows the spread of the residual radial stresses along the height of the rectifying element for different radial cross-sections.

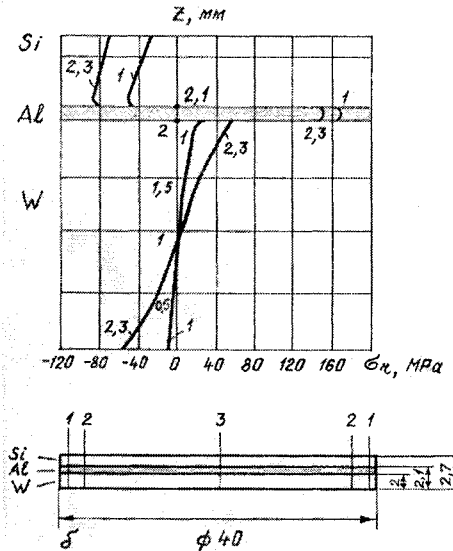


Figure 7: The residual radial stress ( $\sigma_r$ ) in different sections of rectifying element.

## 312 *Surface Treatment VI*

For silicon the residual stresses across the all sections are compressive character. In tungsten the stresses reverse their sign near the middle of height of the layer, which concludes in the bending of the rectifying element.

As shown in Fig. 8, the radial and circular stresses in silicon on the bonded face are close to constant value along the whole radius, but near the edge side of the rectifier the stress value sharply decreases. The tangential and normal stresses in silicon are negligible along the whole radius with the exception of periphery regions of the rectifier.

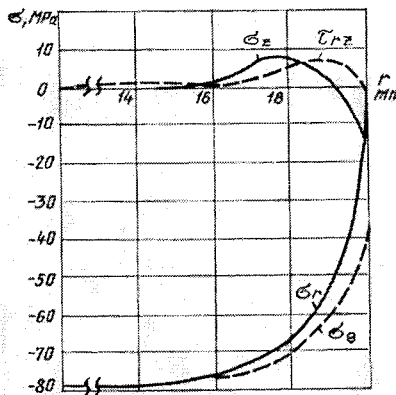


Figure 8: The residual stresses along the radius in bonded face of silicon.  
( $\sigma_r$ ) – radial, ( $\sigma_\theta$ ) – circular, ( $\sigma_z$ ) – normal, ( $\tau_{rz}$ ) – tangential

The results obtained from FEM simulations form the base of following preliminary conclusions:

- In the after bonding cooling process the values of stresses and bending flexure change the sign.
- The residual stresses and deformation of rectifying element have maximum value.
- Despite the bending deformation of rectifying element, the majority of silicon area is under the plane compressive stress and only in a narrow periphery zone silicon is bulk stressed.
- The stress and strain situation in tungsten is close to classic bend, and deformation behavior of tungsten during the whole after bonding cooling process is dominating for the full construction.

## 4 Analytical solution

The FEM calculations give reasonably exact and acceptable issues, which are in a good agreement with the experimental results. Nevertheless, the FEM stays to be

comparatively complicated method for first approximation analysis in quick engineering exercises. In paper [3] Karkhin et. al. suggested a simple two equation analytical solution for stress calculations, which bases on theory of thermo-elasticity for plate like cylindrical configurations.

$$\left\{ \begin{aligned} p \frac{1}{2} \sum_{i=1}^{n_i} D_i (Z_{i+1}^2 - Z_i^2) + q \sum_{i=1}^{n_i} D_i (Z_{i+1} - Z_i) &= \sum_{i=1}^{n_i} C_i \varepsilon_i^T (Z_{i+1} - Z_i) - \sum_{j=1}^{n_j} C_j \sigma_{yj} (Z_{j+1} - Z_j) \\ p \frac{1}{3} \sum_{i=1}^{n_i} D_i (Z_{i+1}^3 - Z_i^3) &= q \frac{1}{2} \sum_{i=1}^{n_i} D_i (Z_{i+1}^2 - Z_i^2) \\ &= \frac{1}{2} \sum_{i=1}^{n_i} C_i \varepsilon_i^T (Z_{i+1}^2 - Z_i^2) - \frac{1}{2} \sum_{j=1}^{n_j} C_j \sigma_{yj} (Z_{j+1}^2 - Z_j^2) \end{aligned} \right. \quad (1)$$

where  $p$  is rotation,  $q$  is radial shift,  $z_i$  is the coordinate of the elastic layer;  $z_j$  is the coordinate of the plastic layer,  $n_i$  is the number of elastic layers;  $n_j$  is the number of plastic layers,  $\varepsilon_i^T$  is thermal expansion coefficient of  $i$ -th layer, and  $\sigma_{yj}$  is the yield stress of  $j$ -th layer.

$$\begin{aligned} D_i &= 2(\mu + \lambda); & C_i &= 3\lambda + 2\mu \\ \mu &= E/2(1 + \nu); & \lambda &= \nu E/(1 + \nu)(1 - 2\nu) \end{aligned} \quad (2)$$

where  $E$  is Young's modulus and  $\nu$  is the Poisson coefficient.

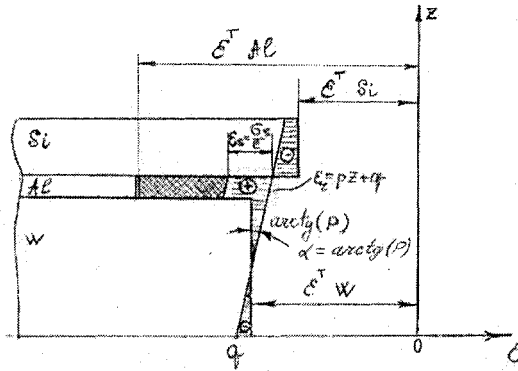


Figure 9: Graphical idea of the analytical solution.

The solution of the equation (1) for  $p$  and  $q$  determines the deformation  $\varepsilon^T$  and corresponding  $\varepsilon_\theta$ ,  $\sigma_r$ , and  $\sigma_\theta$  for every part of the rectifying element. The graphic idea of the approximate analytical solution is shown in Fig. 9.

314 *Surface Treatment VI*

The comparison of the results from FEM and the further described analytical method is shown in Figures 10–13, where the dependences for residual stresses and deformations versus tungsten and aluminium thickness are presented.

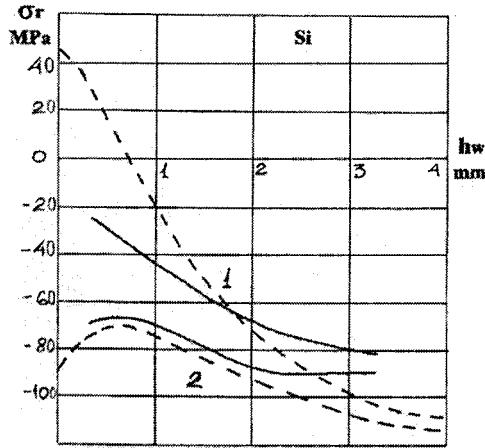


Figure 10: Residual radial stresses on the top (1) and bonded (2) faces of silicon vs. tungsten thickness ( $h_w$ )  
———— FEM solution  
----- analytical solution

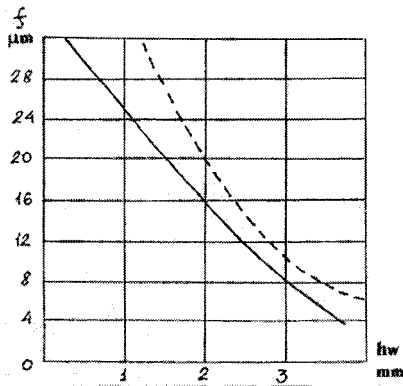


Figure 11: Bending flexure of rectifying element ( $f$ ) dependence on tungsten thickness ( $h_w$ ).  
———— FEM solution  
----- analytical solution



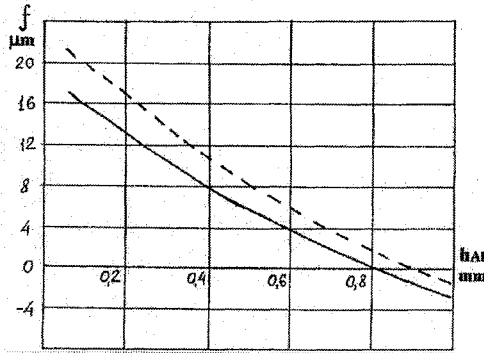


Figure 12: Bending flexure of rectifying element ( $f$ ) dependence on aluminium thickness ( $h_{Al}$ ).

———— FEM solution  
----- analytical solution

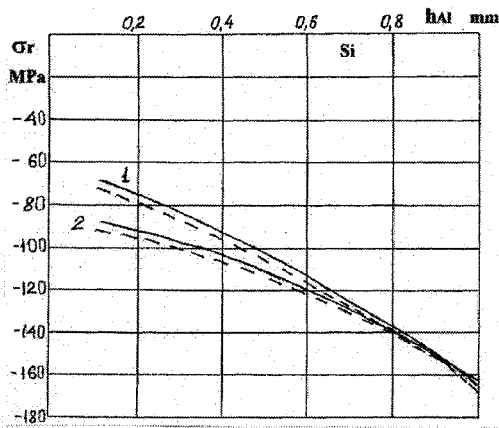


Figure 13: Residual radial stresses on the top (1) and bonded (2) faces of silicon vs. aluminium thickness ( $h_{Al}$ ).

———— FEM solution  
----- analytical solution



## 5 Conclusion

This paper summarizes how to use FEM and analytical techniques for stress analysis in power semiconductor structures. The conclusions, what we present on the base of our results are:

- During the after bonding cooling process, and due to the difference in the thermal coefficients of bonded materials, the stresses and deformations generally rise in the rectifying element. Over the whole cooling process the stresses and deformations change their sign and value at certain ambient temperature, which concludes after this temperature change point in monotonous increase of their values up to the room temperature. The residual values of stress and deformation are the maximums.
- Changing the thickness of electrode and/or connective metal, the stresses and deformation in rectifying element can be directed into proper relation (stress and strain specific optimal solution).
- The diffusion welding process allows to control completely after bonding cooling stress and strain situation. The unique character of the DW process (solid state bonding, based on the surfaces-chemical reactions) removes a series of technology and physics based limitations, which are typical for traditional metallization methods.

Thus, FEM coupled with analytical solution opens an approved practice for novel designs and improvements as well in power semiconductor rectifier production.

## Acknowledgement

The Estonian Science Foundation (grant 4869), and Clifton Ltd. is acknowledged for financial support by investigations resulted in this particular theoretical paper.

## References

- [1] S.B. Dunkerton, Diffusion bonding of materials, *Welding and Metal Fabrication*, pp. 133-136. April 1991.
- [2] O. Korolkov, T. Rang, The diffusion welded contacts in power electronics, In *Proc. 4<sup>th</sup> Baltic Electronics Conference (BEC'94)*, Tallinn, Estonia, pp. 573-578, Oct. 9-14, 1994.
- [3] V. Karkhin, A. Negoda, E. Khutoryansky. and O. Korolkov, The stress and strain kinetics for rectifying element, *Soviet E.P. Conversion Techniques*, issue 3, 1981 (in Russian).